IEEE Access
Multidisciplinary | Rapid Review | Open Access Journal

Received April 30, 2020, accepted May 13, 2020, date of publication May 19, 2020, date of current version June 3, 2020.

Digital Object Identifier 10.1109/ACCESS.2020.2995639

A Two-Phase Stowage Approach for Passenger-Cargo RoRo Ship Based on 2D-KP: Coping With Complex Rotation and Safe Navigation Constraints

YU ZHANG[1,2], HONGWEI TIAN[1], LIJUN HE[1], SHAOKANG MA[1,3], AND LIJUAN YANG[1]

[1]School of Logistics Engineering, Wuhan University of Technology, Wuhan 430063, China
[2]Department of Logistics Engineering and Management, Fujian University of Technology, Fuzhou 350108, China
[3]CCCC Second Harbour Engineering Company Ltd., Wuhan 430071, China

Corresponding author: Lijun He (helj@whut.edu.cn)

This work was supported in part by the National Natural Science Foundation of China under Grant 71874132, and in part by the Fundamental Research Funds for the Central Universities under Grant 2019-YB-033.

ABSTRACT The passenger-cargo Roll on/Roll off ship stowage (PRSS) is the core step of passenger-cargo Roll on/Roll off (RoRo) transportation. The layout of vehicles in the cabin is directly related to the space utilization of the cabin and the efficiency of stowage operations, which in turn affects the economic benefits of the port. In this paper, we address the PRSS problem in the context of passenger-cargo RoRo transportation in the Qiongzhou Strait of China. By focusing on the utilization ratio of the cabin area, the PRSS problem can be viewed as a special version of a two-dimensional knapsack packing (2D-KP) problem with additional constraints, such as two-phase, complex rotation and safe navigation constraints. Then we present a mixed integer linear programming (MILP) mathematical model and an algorithm framework to tackle the PRSS problem. In the algorithm framework, a novel multi-phase heuristic stowage method is proposed to improve the current manual stowage decision-making state which completely depends on operational experience. Finally, several instances are generated based on the realistic date of Qiongzhou Strait to verify the effectiveness of the model and stowage method. Computational results show that the proposed model and stowage method are well suited to solve the PRSS problem and the algorithm framework has a strong robustness in large-scale application experiments.

INDEX TERMS Maritime transportation, ship stowage planning, passenger-cargo roll-on/roll-off, two-dimensional knapsack packing, multi-phase heuristic.

I. INTRODUCTION

Roll on/Roll off (RoRo) ships usually transport cargo on wheels such as cars, trucks, farming equipment, and military equipment [1]. In China, general RoRo ships are mostly used for long-distance mass transportation of commercial vehicles, farming equipment, etc. which have the characteristics of few types, large batch and similar specifications. While passenger-cargo RoRo ships are mainly used for short-distance transportation of sea-crossing vehicles and passengers in coastal areas, among which sea-crossing vehicles include cars, trucks, buses, etc. with multiple types, large numbers, and great differences in specifications. We take passenger-cargo RoRo transportation in Qiongzhou Strait of China, one of the busiest Straits in the world, as an example to show the essential role of passenger-cargo RoRo ship in circulation of passengers and goods between ports across the Strait. Fig. 1(a) shows the geographical location of Qiongzhou Strait, which is the only channel connecting the mainland and Hainan Island of China. In recent years, with the increasing prosperity of tourism and commerce in China, the sea-crossing vehicle and passenger transport volume of passenger-cargo RoRo ships in Qiongzhou Strait have repeatedly set new records, as shown in Fig. 1(b).

During the passenger-cargo RoRo transportation in Qiongzhou Strait, the stowage of passenger-cargo RoRo ship

The associate editor coordinating the review of this manuscript and approving it for publication was Sun-Yuan Hsieh.

This work is licensed under a Creative Commons Attribution 4.0 License. For more information, see https://creativecommons.org/licenses/by/4.0/

(a) Geographical location of Qiongzhou Strait

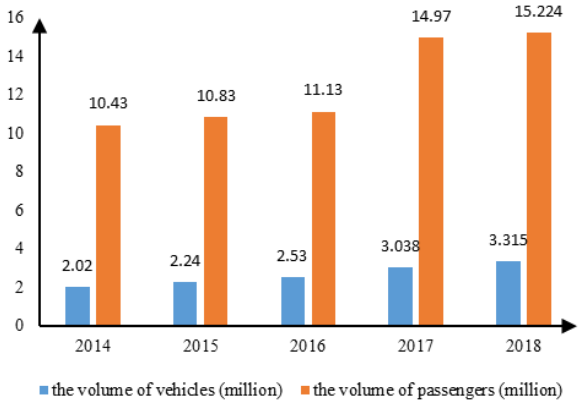

(b) The transport date of passenger-cargo RoRo ship

FIGURE 1. Geographical location of Qiongzhou Strait and the transport date of passenger-cargo RoRo ship.

directly affects the shipping efficiency and port benefits. The type, size, weight and other attributes of sea-crossing vehicles are quite different, and even some super-long and over-heavy-duty trucks are included, making the actual loading decision-making extremely difficult. The current manual ship stowage based on operational experience lacks quantitative assessment indicators. In actual operations, it often needs to be adjusted several times and to make temporary decisions to assist the stowage process, which greatly affects the stowage efficiency and the transportation safety of ships. Given the growing demand of sea-crossing vehicle and passenger transport in Qiongzhou Strait, a fast and efficient stowage decision-making method and intelligent stowage software are urgently needed to improve stowage efficiency of passenger-cargo RoRo transportation.

To the best of our knowledge, there is rare research on passenger-cargo RoRo ship stowage. The existing studies on ship stowage mainly focus on container ships, general cargo ships and general RoRo ships. Among them, scholars are keen on the container ship stowage. Kroer *et al.* [2] proposed two approaches based on binary decision diagrams solvers to solve the container ship stowage problem in a single-bay section. Monaco *et al.* [3] studied the container ship stowage problem considering the terminal management. Li *et al.* [4]–[6] proposed several heuristic algorithms and mathematic models to separately deal with the stowage planning for inland container liner shipping. Zhao *et al.* [7] applied the MCTS (Monte Carlo Tree Search) to container ship stowage solution for the first time and created a generating algorithm accordingly. Zhang *et al.* [8] and Wei [9] regarded container ship stowage problem as a two-dimensional (2D) bin-packing problem, and adopted the packing approaches to solve the issue. Sciomachen and Tanfani [10] further analyzed the connection between the container ship stowage problem considering the master bay and the bin packing problem. There also has been little research on the ship stowage planning problem for steel cargoes. Umeda *et al.* [11] used simulated annealing (SA) algorithm to solve the ship stowage problem of steel products. In Tang *et al.* [12], the stowage problem where the steel coils without fixed positions on the ship was considered, and a mixed integer linear programming (MILP) model and a tabu search algorithm is developed for the problem. On the RoRo transportation, stowage problem also plays a key role. Nevertheless, the relevant research is very rare. In Øvstebø *et al.* [1], [13], the stowage planning of general RoRo ship is concerned, while the specific location of vehicles in ships is neglected. The idea of applying 2D packing theory to general RoRo ship stowage has only been concerned in [14], where a stowage model and a shifting model are presented to solve the stowage problem in RoRo liner shipping.

The above three kinds of ship stowage problems have certain common characteristics, such as: a) they must meet the stability constraints and load limits to ensure the navigation safety of the ship, and b) all of them need to consider cargo handling constraints to facilitate the rapid loading and unloading operations at the destination port. Nevertheless, each type of those problems has its own uniqueness. In the stowage problem of container ships and general cargo ships, containers or general cargoes are stacked in layers in the vertical direction, and the loading and unloading operations are carried out directly by the corresponding lifting equipment. In contrast, in the case of RoRo ship stowage, the ship has multi-deck structure, and vehicles are driven directly into the cabin without any loading and unloading equipment. Furthermore, there are also many differences between general RoRo ship stowage (GRSS) and passenger-cargo RoRo ship stowage (PRSS), detailed in Table 1. It is worth noting that, in GRSS problem, vehicles belonging to the same shipment should be placed intensively and parked neatly along the lane so as to ease the loading/unloading at a given port, as shown in Fig. 2(a). In this way, based on the rated load capacity of a ship and the total length of the lane divided by the cabin, the loading degree of the cabin can be determined by measuring the total length and weight of the loaded vehicle, which is relatively easy to measure. However, in PRSS problem, as there is normally only one destination port, in order to make full use of the cabin area to improve the transportation

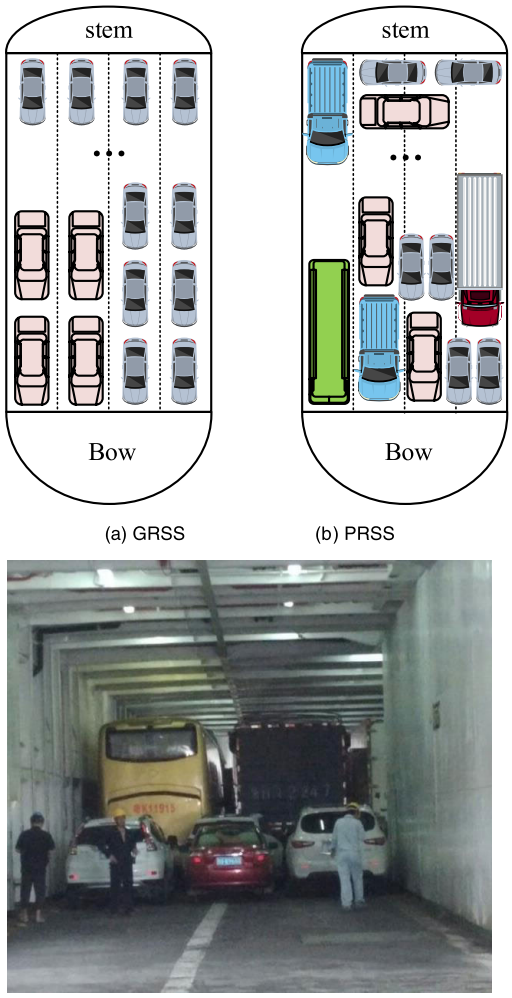

(a) GRSS (b) PRSS

(c)The scene of PRSS

FIGURE 2. Illustration of the GRSS and PRSS.

efficiency, it is not necessary for vehicles to be placed exactly along the lane. In addition, there are two stowage phases in PRSS, and the selection criteria and the parking freedom degree of vehicles vary at different phases. As illustrated in Fig. 2(b), some vehicles with small turning radius are allowed to rotate 90 degrees in the stern area.

In the PRSS problem, it is assumed that the cabin is a large rectangular bin, and the sea-crossing vehicles are rectangular items. Then, the stowage problem can be regarded as a packing problem. Since the vehicle loaded in the cabin cannot be stacked vertically, the problem can be further considered as a two-dimensional (2D) rectangular packing problem. Specifically, the classical 2D rectangular packing problem can be divided into three sub-problems, namely two-dimensional strip packing (2D-SP), two-dimensional bin packing (2D-BP) and two-dimensional knapsack packing (2D-KP) [15], [16]. Each of them can be further divided into four classes according to whether the rotation and guillotine are required [17]. Major classes of two-dimensional rectangular packing problems are detailed in Table 2. One aim of the PRSS problem is to pack a part of arrived vehicles into the cabin efficiently within a certain period, which is close to that of the 2D-KP problem. Moreover, the PRSS problem also has its own stowage features, such as two-phase and complex rotation. PRSS problem therefore can be regarded as an extended 2D-KP problem.

To dates, the study on 2D-KP method has been relatively mature. A hybrid SA algorithm in [18] was proposed to solve the 2D-KP problem. The algorithm used an adaptive strategy to score the placed rectangles for constructing the initial solution, and applied the SA algorithm to optimize the solution. Shiangjen *et al.* [19] proposed an enhanced heuristic placement algorithm, which was used to increase the feasibility for packing more suitable items to a container by improving the packing rules in [18]. Wei *et al.* [20] proposed an improved best-fit heuristic algorithm based on the algorithm presented in [21] for 2D-KP problem. The optimal placement was obtained by scoring rectangular items placed in the gap, and a random local search was used to find the better packing sequence. Zhou *et al.* [22] studied the 2D-KP problem with block packing constraints. In [23]–[25], the 2D multiple knapsack problem in different scenarios were discussed, respectively.

Note that RF means 90-degree rotation is allowed but the guillotine is not required, RG means 90-degree rotation is allowed and the guillotine is required, OF means rotation is not allowed and the guillotine is not required, and OG means rotation is not allowed but the guillotine is required. Here, ''guillotine'' means that each cut must be able to divide the original rectangle into two rectangles.

From these reviews, we conclude that our PRSS problem has several special characteristics. First, the PRSS problem is quite different from the stowage problems of container ship, general cargo ship and general RoRo ship. Existing stowage decision-making methods are difficult to directly apply in the field of PRSS. Therefore, it is necessary to design a new stowage decision model and solution method that fits the actual operation of PRSS. Second, considering the packing characteristics in the process of the PRSS, this paper regards the PRSS problem as an extended 2D-KP problem, which belongs to the NP-hard problem. Therefore, in large-scale stowage problems, it is difficult for manual decision-making methods to obtain a better stowage plan in a limited time. An intelligent optimization method is needed to solve this problem. Third, the PRSS problem contains four out of the ten categories of constraints summarized by Bortfeldt and Wäscher [26]. Only 16% of the articles in their review consider more than three constraints [27]. Hence our problem is highly constrained.

The main contributions of this work are summarized as follows:

(1) This work firstly addresses a PRSS problem with the consideration of two-dimensional packing, safe navigation, two-phase and complex rotation characteristics. In view of the characteristics, a MILP model is proposed to tackle the problem.

TABLE 1. Differences between PRSS and GRSS problems.

Difference	PRSS	GRSS
Ship structure	The ship with multi-deck structure, in which the upper decks are passenger cabins and the lower decks are used for loading vehicles. In China, the ship normally uses a single deck to load vehicles.	The ship with multi-deck structure, and all decks are used for loading vehicles.
Service objects	Services for social crossing vehicles, such as trucks, cars, buses and even some super-long and over-heavy-duty trucks, which vary greatly in size and weight.	Most of the service objects are commodity vehicles with similar specifications.
Stowage features	a) There are two stowage phases. Vehicles arriving at different phases are treated differently, and the parking freedom degree of vehicles varies at different phases. b) It is not necessary for vehicles to be placed along the lane as there is normally only one destination port. c) The length and width of vehicles should be considered during the stowage process.	a) There is no difference in the service order. b) Vehicles are usually placed neatly in categories along the lane so as to ease the loading/unloading at a given set of ports. c) The width of vehicles can be neglected in most cases due to the stowage characteristics.

TABLE 2. Major classes of two-dimensional rectangular packing problems.

Basic problems	2D-SP	2D-BP	2D-KP
Classification	RF RG OF OG	RF RG OF OG	RF RG OF OG
Description	The sheet with fixed width and infinite length. The goal is to pack all items with the lowest height.	The sheet with fixed width and length. The goal is to pack all items with the least number of sheets.	The sheet with fixed width and length, and each item has its corresponding value. The goal is to pack a part of the items with the greatest value.

(2) A biased random key hybrid algorithm (BRKHA) framework is proposed to handle the problem. Several effective operators are adopted to improve the performance of proposed BRKHA, including biased random key based encoding, multi-phase heuristics, fitness evaluation and evolutionary operations.
(2) Simulation experiment and application experiment including large number of instances are generated to test the feasibility of the MILP model as well as the BRKHA framework. Three widely used swarm intelligence algorithms are applied separately in the evolutionary operation of the framework as a result comparison.

The rest of the paper is organized as follows. Section II introduces the PRSS problem. The MILP mathematical model is constructed in Section III. The algorithm framework and heuristic methods for PRSS are described in Section IV. The experimental results and analysis are reported in Section V, followed by conclusions and research prospects that are provided in Section VI.

II. PROBLEM DESCRIPTION

The intelligent management system of passenger-cargo RoRo transportation in Qiongzhou Strait is in the stage of research and development, while the matching intelligent stowage decision-making method eagerly needs to be resolved. In the intelligent management system, passengers or vehicle owners make online reservations for ticket purchase in advance, and the port dispatching center formulates the berth planning for the waiting area and the stowage planning for each ship based on the reservation information, as illustrated in Figure 3. This paper focus on the problem of PRSS planning, which is mainly oriented to the passenger-cargo RoRo coastal transportation with the characteristics of single voyage (there are no other ports between origin and destination), high flow of people, large traffic, multi-type vehicles and efficient transportation demand.

The 2D-KP problem is one of the most classical problems in the combinatorial optimization field and has a lot of applications in the real world [28]. In the 2D-KP problem, each item has a corresponding profit, and one needs to select a subset of items to be packed in a single bin to maximize the total profit of selected items [22]. Similar to the objective of the 2D-KP problem, the PRSS problem aims to pack a part of arrived vehicles into the cabin efficiently within a certain period to maximize the cabin area utilization, thereby improving transportation efficiency. We therefore consider tackling the PRSS problem based on the 2D-KP theory.

First of all, the characteristics of PRSS are the key to analyze the studied problem. They include two-dimensional packing, safe navigation, two-phase and complex rotation. Details of these characteristics are presented as follows.

A. TWO-DIMENSIONAL PACKING

During the stowage planning, as shown in Fig. 4(a), the cabin and sea-crossing vehicles can be regarded as a rectangular sheet and rectangular items, respectively. The PRSS problem can be regarded as a problem that needs to select a subset of rectangular items to be packed in a rectangular sheet under specific stowage constraints to maximize the area utilization

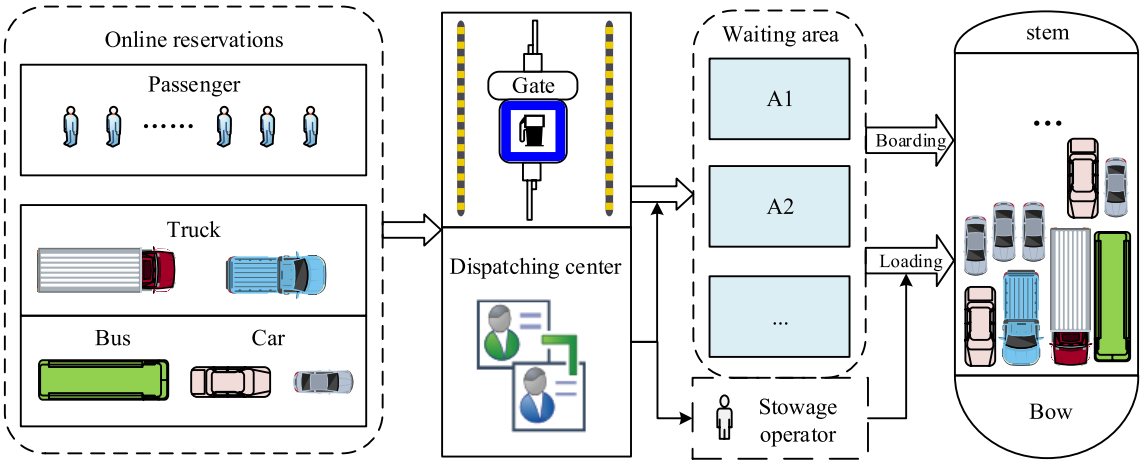

FIGURE 3. The formulation process of PRSS planning.

of the sheet. Such problem can be regarded as a 2D-KP problem with the particular constraints.

B. SAFE NAVIGATION

In order to ensure the navigation safety of the passenger-cargo RoRo ship, the practical constraints such as ship stability and safe distance between vehicles should be considered. In terms of ship stability, it is required that the ship's longitudinal and horizontal moment and total weight should be maintained within the rated range. For the safety distance, it is necessary to leave a certain distance between not only vehicles but also the vehicle and the cabin bulkhead in order to reserve the operation space for operator and ensure the safety of vehicles, as illustrated in Fig. 4(b).

C. TWO-PHASE

In actual port operations, with 80% of the cabin length as the critical point, the stowage process in Qiongzhou Strait is usually divided into two phases. Vehicles arriving at different stowage phases are treated differently, and the loading sequence is not strictly first-come-first-served as the stability of the cabin needs to be considered first. Specifically, during the early phase, there is sufficient remaining area in the cabin. It is necessary for the port to pack all arriving vehicles into the cabin in a sequence that facilitates the utilization of the cabin area, and we call this phase the main stowage planning phase (MSPP). In the later phase, due to the limited remaining area of the cabin, the stowage operator has to select some vehicles into the cabin until the total weight of packed vehicles reaches 90% of the cabin's rated load or the cabin is full. Correspondingly, this phase is called supplemental stowage planning phase (SSPP).

D. COMPLEX ROTATION

During the loading process, the vehicle enters the cabin from the stern and occupies the bow area preferentially. In MSPP, considering the space limitation and unloading difficulties, vehicles are not allowed to rotate, and the stowage problem in this area only has the OF characteristic of the 2D-KP. In SSPP, the space limitation and unloading difficulties are alleviated. As shown in Fig. 4(b), small vehicles with small turning radius are allowed to rotate 90 degrees flexibly, while large vehicles such as trucks and buses are limited by the turning radius and are still non-rotatable. In this area, the stowage problem of small vehicles has both RF and OF characteristics of the 2D-KP problem, but that of large vehicles has only OF characteristic.

III. MATHEMATICAL MODEL

A. ASSUMPTIONS

Due to the "Roll on/Roll off" nature of passenger-cargo RoRo ship, the stowage time is far less than the ship's dwell time in port. This paper does not consider the stowage time constraints. The assumptions for the PRSS are presented as follows:

1) The coordinate system is established in the lower left corner of the cabin stowage area.

2) It is assumed that the cabin and vehicles are rectangular with uniform mass.

3) Assuming that the number of vehicles to be packed is larger than the maximum capacity of the cabin and the vehicle data is known.

B. MILP MODEL

Notations:

I : Set of vehicles, $I = \{i|i = 1, 2, \cdots, |I|\}$. The serial numbers are numbered in order of arrival.

I_s : Set of cars.

I_b : Set of trucks and buses, $I_b = I - I_s$.

I_1 : Set of vehicles at MSPP, $I_1 = \{i|i = 1, 2, \cdots, |I_1|\}$.

I_2 : Set of vehicles at SSPP, $I_2 = I - I_1$.

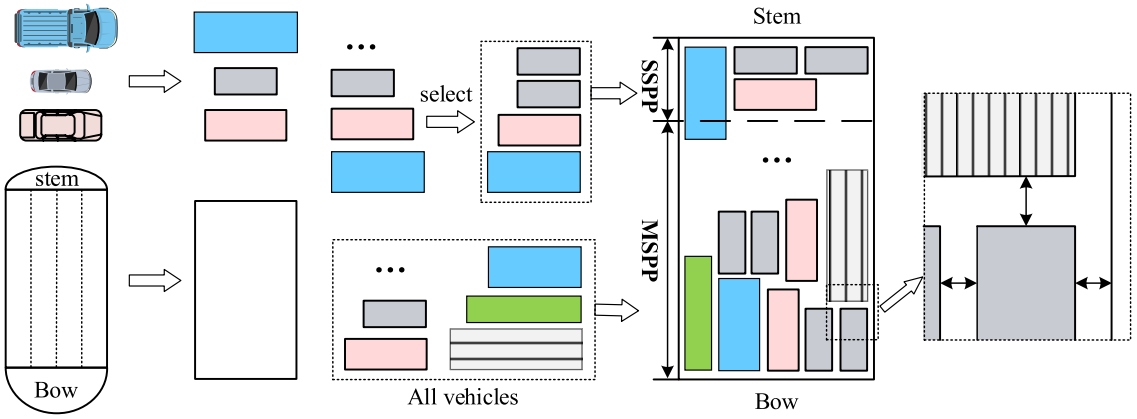

FIGURE 4. Characteristic diagram of PRSS problem.

W, L : The width and length of the passenger-cargo RoRo ship.

d_x, d_y : The safety distance in direction of x-axis and y-axis.

$\overline{w_i}$, $\overline{l_i}$: The original width and length of the vehicle i.

w_i, l_i : The width and length of the vehicle i containing the safety distance.

m_i : The mass of vehicle i.

M : An arbitrarily large number.

G : The rated load capacity of the ship.

T_x : The maximum horizontal moment of the ship in the x-axis direction.

T_y : The maximum longitudinal moment of the ship in the y-axis direction.

Variables:

(x_i, y_i) : Integer variables that define the x and y coordinates of vehicle i in the ship.

z_{ij} : Binary variable. If vehicle i is on the left of vehicle j, that is $x_i + w_i \le x_j$ or $x_i + l_i \le x_j$, $z_{ij} = 1$; otherwise, $z_{ij} = 0$.

b_{ij} : Binary variable. If vehicle i is below the vehicle j, that is $y_i + l_i \le y_j$ or $y_i + w_i \le y_j$, $b_{ij} = 1$; otherwise, $b_{ij} = 0$.

s_i : Binary variable. If vehicle i is placed in the cabin, $s_i = 1$, otherwise, $s_i = 0$.

$\overline{r_i}$: Binary variable. If vehicle i is allowed to be placed in rotation, $\overline{r_i} = 1$; otherwise, $\overline{r_i} = 0$.

r_i : Binary variable. If vehicle i is placed in rotation, $r_i = 1$; otherwise, $r_i = 0$.

Objective Function:

The aim of the PRSS problem is to maximize the utilization of the cabin area. In this work, the objective function is presented as follows:

$$f = \max \sum_{i \in I} s_i l_i w_i / LW \tag{1}$$

Constraints:

The constraints are divided into four categories: two-dimensional packing characteristic constraints, two-phase characteristic constraints, rotation characteristic constraints and safety navigation characteristic constraints. Details of these constraints are presented as follows.

Two-dimensional packing characteristic constraints. Constraints (2)-(6) ensure that none of the placed vehicles overlaps each other. According to the characteristics of the problem, the trucks and buses are not allowed to be placed in rotation, and the cars can be placed in rotation. Constraints (7)-(10) guarantee that all vehicles must be placed inside the dimensions of the cabin.

$$z_{ij} + z_{ji} + b_{ij} + b_{ji} + (1 - s_i) + (1 - s_j) \ge 1, \quad \forall i \ne j, i, j \in I \tag{2}$$

$$x_i + r_i l_i + (1 - r_i) w_i \le x_j + M(1 - z_{ij} + 2 - s_i - s_j), \quad \forall i \ne j, i \in I_s, j \in I \tag{3}$$

$$y_i + r_i w_i + (1 - r_i) l_i \le y_j + M(1 - b_{ij} + 2 - s_i - s_j), \quad \forall i \ne j, i \in I_s, j \in I \tag{4}$$

$$x_i + w_i \le x_j + M(1 - z_{ij} + 2 - s_i - s_j), \quad \forall i \ne j, i \in I_b, j \in I \tag{5}$$

$$y_i + l_i \le y_j + M(1 - b_{ij} + 2 - s_i - s_j), \quad \forall i \ne j, i \in I_b, j \in I \tag{6}$$

$$x_i + r_i l_i + (1 - r_i) w_i \le W + M(1 - s_i), \quad \forall i \in I_s \tag{7}$$

$$y_i + r_i w_i + (1 - r_i) l_i \le L + M(1 - s_i), \quad \forall i \in I_s \tag{8}$$

$$x_i + w_i \le W + M(1 - s_i), \quad \forall i \in I_b \tag{9}$$

$$y_i + l_i \le L + M(1 - s_i), \quad \forall i \in I_b \tag{10}$$

Two-phase characteristic constraints. Constraint (11) ensures that all vehicles at MSPP must be placed in the cabin and part of vehicles at SSPP is selected to be placed. $|I_1|$ is uniquely determined by inequality (12).

$$s_i = 1, \quad \forall i \in I_1 \tag{11}$$

$$\sum_{i=1}^{|I_1|} l_i w_i \le 0.8LW < \sum_{i=1}^{|I_1|+1} l_i w_i \tag{12}$$

Rotation characteristic constraints. Constraints (13) to (15) represent the relationship between $\overline{r_i}$ and y_i. If $y_i \ge 0.8L$,

the vehicles are considered to be at the stern of the cabin and the cars are allowed to be placed in rotation, and then $\overline{r_i} = 1$, otherwise $\overline{r_i} = 0$. Constraint (16) denotes the relationship between r_i and $\overline{r_i}$. If the cars are allowed to be placed in rotation, $\overline{r_i} = 1$ and $r_i \in \{0, 1\}$; otherwise $\overline{r_i} = 0$ and $r_i = 0$.

$$M\overline{r_i} - (y_i - 0.8L) \geq 0, \quad \forall i \in I_s \tag{13}$$

$$M\overline{r_i} - (y_i - 0.8L) \leq M, \quad \forall i \in I_s \tag{14}$$

$$\overline{r_i} = 0, \quad \forall i \in I_b \tag{15}$$

$$r_i \leq \overline{r_i}, \quad \forall i \in I_s \tag{16}$$

Safety navigation characteristic constraints. Constraint (17) guarantees that the total load of the ship does not exceed 90% of its rated load. Constraints (18) and (19) ensure that the longitudinal and horizontal moments of the ship are within the rated range.

$$\sum_{i \in I} m_i s_i \leq 0.9G, \quad \forall i \in I \tag{17}$$

$$-T_x \leq \sum_{i \in I} m_i s_i (x_i + (r_i l_i + (1 - r_i) w_i - W)/2) \leq T_x, \quad \forall i \in I \tag{18}$$

$$-T_y \leq \sum_{i \in I} m_i s_i (y_i + (r_i w_i + (1 - r_i) l_i - L)/2) \leq T_y, \quad \forall i \in I \tag{19}$$

Variable definition. Constraints (20)-(23) define the range of variables.

$$x_i, y_i \in N_+, \quad \forall i \in I \tag{20}$$

$$z_{ij}, b_{ij} \in \{0, 1\}, \quad \forall i \neq j, i, j \in I \tag{21}$$

$$s_i \in \{0, 1\}, \quad \forall i \in I \tag{22}$$

$$r_i, \overline{r_i} \in \{0, 1\} \quad \forall i \in I \tag{23}$$

To verify the effectiveness of the model and algorithm, the upper bound model (UBM) of the problem is obtained by relaxing the model constraints. The UBM of the problem is presented as follows:

$$\sum_{i \in I} l_i w_i \leq LW, \quad \forall i \in I \tag{24}$$

$$\text{(UBM)} \left\{ f = \max \sum_{i \in I} s_i l_i w_i / LW : (11), (12), (17), (22), (24) \right\}$$

which relaxes the two-dimensional packing characteristic constraints (2)∼(10), the rotation characteristic constraints (13)∼(16) and the safety navigation characteristic constraints (18)∼(19). Formula (24) indicates that the total area of vehicles does not exceed the cabin area.

IV. ALGORITHM

In this section, a biased random key-based hybrid algorithm (BRKHA) framework is proposed to solve the PRSS problem. The proposed algorithm framework mainly consists of biased random key based encoding, multi-phase heuristics, fitness evaluation and evolutionary operations. Biased random key based encoding [29] generates the vehicles packing sequence. Multi-phase heuristic constructs a ship stowage planning through a given encoding individual and three placement strategies. And the fitness is used to evaluate the quality of the stowage planning scheme. Given the excellent search ability of swarm intelligence algorithm [30], evolutionary operations based on swarm intelligence algorithm are utilized to find the better packing sequence and improve the quality of the solution. Fig. 5 shows the framework of proposed algorithm framework.

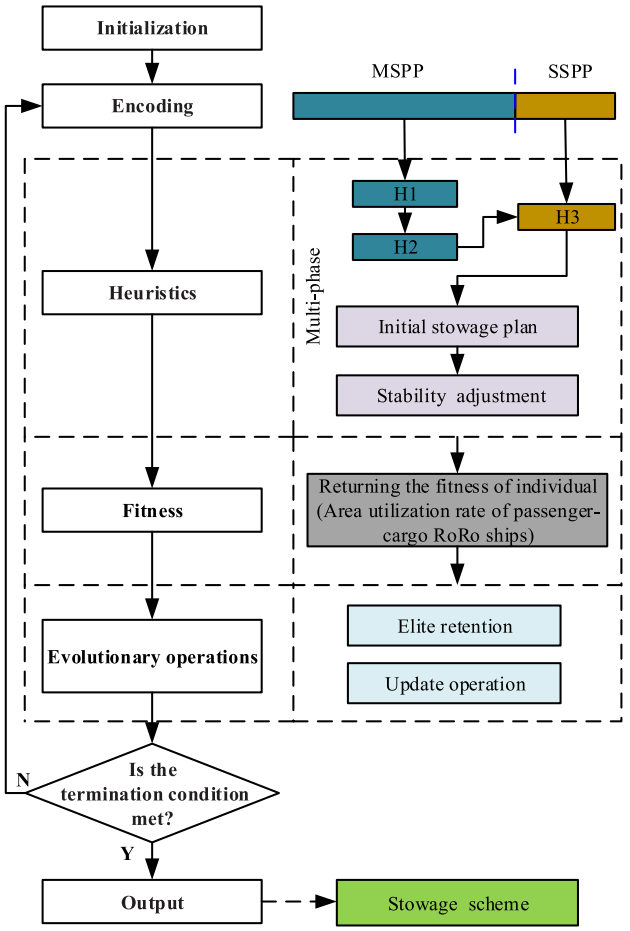

FIGURE 5. Algorithm framework.

A. ENCODING

In our algorithm framework, the encode method uses a string of random keys to represent the packing sequence. The stowage planning is obtained indirectly by the multi-phase heuristic decoding the packing sequence. Each sequence (called individual) consists of $|I|$ random keys and is divided into two phases according to the stowage process. The stowage sequence in two phases is obtained separately by ascending order of corresponding random keys.

Fig. 6 shows the encoding process of an example with the stowage of 5 vehicles. The individual is composed of 5 random keys, each of which corresponds to a vehicle marked with the arrival number. The random keys sort in ascending order to generate the vehicle packing sequence in

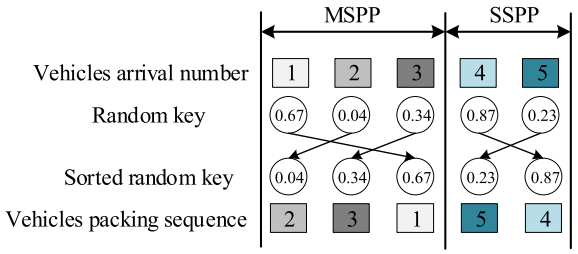

FIGURE 6. Two-phase encoding of vehicles packing sequence.

both stowage phases. The final vehicle packing sequence in Fig. 6 is $2 \rightarrow 3 \rightarrow 1 \,|\, 5 \rightarrow 4$.

Let PS be the population size of the algorithm. Since the encoding operation assigns values to each individual, and there are $|I|$ vehicles, the worst-case computational complexity (CC) of the encoding operation is $O(PS * |I|)$.

B. MULTI-PHASE HEURISTICS

Multi-phase heuristic consists of initial solution construction and stability adjustment. The initial solution construction obtains a stowage planning through three heuristics, which satisfies the two-phase and rotation constraints, including left-right-left stowage for the first layer (H1), main stowage based on scoring strategy (H2) and supplemental stowage (H3). The vehicles interchange strategy is used to change the longitudinal and horizontal moment to meet ship stability requirements.

1) INITIAL SOLUTION CONSTRUCTION

a: LEFT-RIGHT-LEFT STOWAGE FOR THE FIRST LAYER (H1)

The PRSS is more sensitive to horizontal moment than longitudinal moment due to the hull structure feature of passenger-cargo RoRo vessel. It is necessary to control horizontal moment at a small value when packing vehicles to lighten the difficulty of stability adjustment. According to the stowage experience of stowage operators in the port, the distribution of vehicles at the bottom of the cabin (bow) can largely determine the distribution of subsequent vehicles, and then affect the horizontal moment distribution of the ship. Therefore, in order to produce a stowage planning with productive horizontal moment, H1 is designed to achieve the first layer placement at the MPSP and provide a good layout for subsequent stowage.

The key to H1 heuristic is to place similar or identical vehicles symmetrically. Fig. 7 shows an example of the first layer stowage process. In the case, the first step is to search for the vehicle which is similar to vehicle 1 in the sequence. There, vehicle 3 as shown is the most similar to vehicle 1. Since the vehicle 1 is placed on the far left side of the first layer of cabin, the vehicle 3 is placed on the far right side. Likewise, the vehicle 2 is similar to the vehicle 5, and the vehicle 2 is placed next to the vehicle 1, so that the vehicle 5 is placed next to the vehicle 3. When the gap of first layer is unable to accommodate the current two similar vehicles,

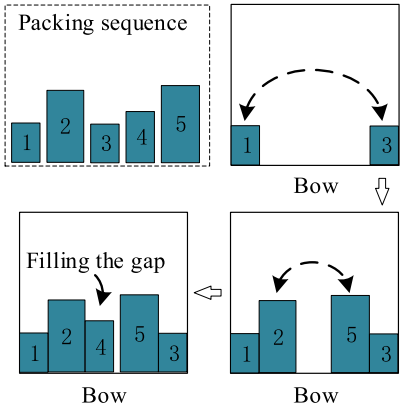

FIGURE 7. An example of stowage for the first layer.

TABLE 3. Scoring strategy of vehicle placement.

Situation A	Situation B	Condition	Score
w_i=w_{ej}	k-1	A and B	3
w_i=w_{ej}	k+1	A and B	2
w_i<w_{ej}	k	A and B	1
w_i<w_{ej}	k+1	A and B	0

the other two or one of the largest vehicles that can be placed in the gap is selected to place in the gap.

b: MAIN STOWAGE BASED ON SCORING STRATEGY (H2)

H2 uses scoring strategy developed by [21] to evaluate the placement of remaining vehicles at MSPP. The stowage surface of cabin is defined based on the skyline in [21]. As shown in Fig. 8(a), the stowage surface formed by packed vehicles can be represented by a sequence $E = \{e_1, e_2, \ldots, e_j, \ldots, e_k\}$. E consists of k horizontal segments counted from left to right with $e_j = \{x_{ej}, y_{ej}, w_{ej}\}$. (x_{ej}, y_{ej}) and w_{ej} respectively represent the left endpoint coordinates and width of e_j. The e_j with the minimum y value becomes the lowest stowage surface and is recorded as $e_{\min}$. The adjacent stowage surface is the segments adjacent to $e_{\min}$ in E. Generally, $e_{\min}$ has two adjacent stowage surfaces. But when $e_{\min}$ is the first or the last in E, there is only one adjacent stowage surface in E. At this time, another adjacent stowage surface is considered to be the edge of the sheet, and its height is the length L of the sheet. The above provides the basis for the H2 process.

While trying to place the vehicle in the cabin, a scoring strategy is used to evaluate the quality of vehicle placement. Table 3 details the scoring strategy, where situation A indicates the matching degree between vehicle width (w_i) and stowage surface width (w_{ej}), and situation B reflects the change in the number of stowage surfaces. A larger score means a higher space utilization degree of the current stowage surface.

The cabin is divided into left and right space along the y axis. The stowage process is mainly as follows:

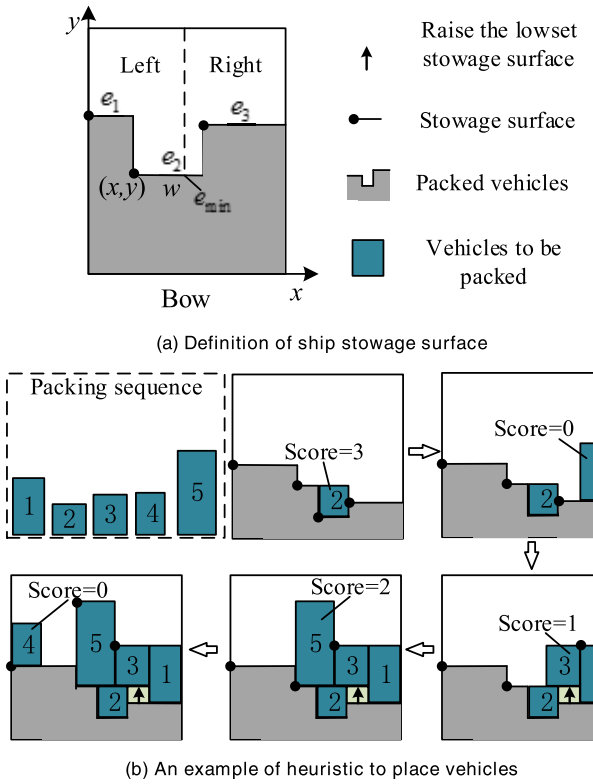

FIGURE 8. Main stowage based on scoring strategy.

- Find out the $e_{\min}$ in the current state and determine its space in the cabin. The x-axis coordinate of the midpoint of $w_{e\,\min}$ is taken as criteria, which means $e_{\min}$ is located in the same space as the coordinate $(x_{e\,\min} + w_{e\,\min})/2$.
- Place the vehicle in $e_{\min}$ or raise the $e_{\min}$. If there are vehicles in the MSPP sequence that can be placed in $e_{\min}$, the vehicle with the highest score will be packed into cabin. When there are several vehicles with the same score, the first arrival vehicle is selected. Otherwise, $e_{\min}$ will be raise to the lowest one in the adjacent stowage surface.
- Update E and repeat the above operation until the total weight of packed vehicles reaches 90% of the cabin's rated load or the cabin is full.

In particular, if a vehicle with the score of 0, the vehicle will be placed on the same side as $e_{\min}$ in the cabin, so that the ship will have a good horizontal moment. Fig. 8(b) is an example of the H2 heuristic placement of vehicles, and the score for each placement are shown in the figure.

c: SUPPLEMENTAL STOWAGE (H3)

At the end of MSPP, with the decrease of the remaining vehicles, the stowage surface may be raised continuously, because it is difficult to ensure that the vehicle to be placed matches the lowest stowage surface. After entering the SSPP, the vehicle set changes and there are a certain number of vehicles that can be placed under the stowage surface which has been raised at MSPP. This will result in a waste of part of the cabin area, as shown in Fig. 9. Therefore, a repairing strategy is designed to avoid this situation. When the MSPP is completed, the raised stowage surface without vehicle placed is returned to the previous state position, and the repaired surface set is used as the initial stowage surface of the SSPP.

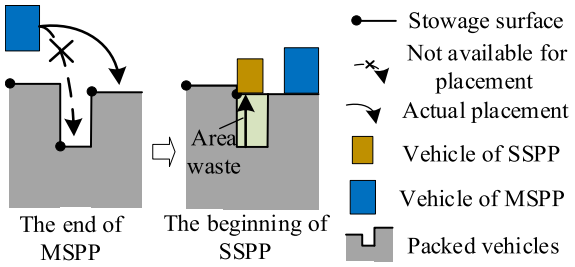

FIGURE 9. Area waste due to phase transition.

The stowage method and placement strategy of MSPP are still used during the SSPP. However, it is worth noting that when the ordinate y of $e_{\min}$ is in the stern range, the available rotation of small vehicles should be considered until the cabin is full, in order to make full use of the cabin area.

2) STABILITY ADJUSTMENT

The longitudinal and horizontal moment of the passenger-cargo RoRo ship are mainly determined by trucks which of greater weight compared with cars and buses. In addition, there are usually trucks of the same size but different weight in the cabin. Therefore, an adjustment strategy is proposed to optimize the longitudinal and horizontal moment without destructive changes to the distribution layout, which is achieved by exchanging trucks with different weight but the same size. If $\overrightarrow{T}_{xy}$ is used to represent the longitudinal and horizontal moment of the stowage scheme, the ideal position of $\overrightarrow{T}_{xy}$ should be (0, 0). The purpose of interchanging trucks is to make $\overrightarrow{T}_{xy}$ as close as possible to the vector (0, 0) so as to meet the stability requirements.

ΔT_x and ΔT_y represent the horizontal and longitudinal moment of the scheme respectively, which can be obtained by formula (18) and (19), and the current stability can be expressed as:

$$\overrightarrow{T}_{xy}=(\Delta T_x, \Delta T_y) \tag{25}$$

For two trucks u and v of the same size, the change of the horizontal and longitudinal moment after interchange can be expressed as follows:

$$\overrightarrow{\Delta T}_{xy}=((x_v - x_u)(m_u - m_v), (y_v - y_u)(m_u - m_v)) \tag{26}$$

Then the overall stability changes to:

$$\overrightarrow{T'}_{xy} = \overrightarrow{T}_{xy} + \overrightarrow{\Delta T}_{xy} = (\Delta T_x + (x_v - x_u)(m_u - m_v), \Delta T_y + (y_v - y_u)(m_u - m_v)) \tag{27}$$

When implementing the interchange strategy, there may be the following situations:

TABLE 4. Experimental vehicle proportions.

scenario	Night			Daytime		
	Truck	Car	Bus	Truck	Car	Bus
P1	0.7	0.3	0	0.4	0.5	0.1
P2	0.6	0.4	0	0.3	0.6	0.1

TABLE 5. Attributes of passenger-cargo RoRo ships.

Ship	Length /m	Width/ m	Load capacity/t	Maximum horizontal moment / kN□m	Maximum longitudinal moment / kN□m
V1	22	4	55	600	3300
V2	62	9	650	1350	9300
A1	88	16	980	2400	13200
A2	116	18	1900	2700	17400
A3	124	18	2704	2700	18600

TABLE 6. Types and data of vehicles.

Vehicle type		Vehicle category	length/m	width/m	weight/t
Truck	General truck	Van	8.0	2.5	4.9~8.5
		Refrigerated truck	8.6		7.8~15.8
		Barrier truck	9.0		5.8~16.0
		Dump truck	9.1		8.0~16.0
		Fence truck	12.0		10.0~31.0
	Flatbed truck		11.9	2.5	11.4~28.0
	Semitrailer		12.5		4.5~38.0
	Container truck	20 ft.	9.5	2.6	20.0~28.0
		40 ft.	13		25.0~40.0
Car	Microbus		4.5	1.7	1.3
	Sedan car		4.6	1.8	1.2
	MPV		4.7	1.8	1.5
	SUV		5.1	2.0	2.2
Bus	Minibus		7.2	2.2	5.7
	Large bus		8.7	2.5	9.0

① If there are several groups of trucks that can be interchanged, the two vehicles whose vector $\overrightarrow{T'}_{xy}$ after the interchange is more close to the ideal position than other groups are selected to perform the interchange operation.

② If the vector $\overrightarrow{T'}_{xy}$ deviates from the ideal position more than $\overrightarrow{T}_{xy}$, then the interchange is cancelled.

The heuristic stops when the stowage scheme meets the stability requirements or no vehicle can be used for interchange. If the heuristically adjusted stowage scheme still does not meet the stability requirements, the scheme is abandoned.

In multi-phase heuristics, the vehicle search process needs to search $(|I|-1)+(|I|-2)+(|I|-3)+\cdots+1 = |I|(|I|-1)/2$ times in the worst case, where $|I|$ is the number of vehicles. Thus, the worst-case CC of the multi-phase heuristics is $O(PS*|I|^2)$.

C. FITNESS AND EVOLUTIONARY OPERATIONS

Fitness is used to evaluate the quality of heuristic stowage scheme. In this paper, the area utilization ratio of the stowage scheme is taken as the fitness, which is obtained by the objective function of the MILP model.

The evolutionary operation is used to search for the better solution, including elite retention and update operation. Elite retention preserves the best individuals that have emerged so far in the evolutionary process to the next generation, ensuring that the best solution is not destroyed by other operations. In the update operation, the search mechanism based on swarm intelligence algorithm is considered in this paper.

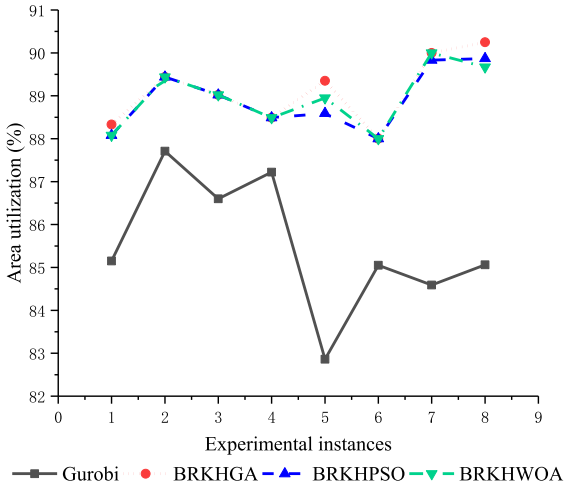

FIGURE 10. Visual comparison of ship V2 stowage area utilization.

The search operation of genetic algorithm (GA) is taken as an example to illustrate the evolutionary operations of proposed algorithm framework. The update mode of GA refers to [29] including crossover and mutation operations. It selects individuals randomly from the elite and non-elite groups for crossover firstly. In the process of crossover, the random key element is used as the operation object, and the corresponding elements of the two chromosomes are selected according to the crossover probability ρ_e to be transmitted to the next generation. The mutation operation randomly generates multiple individuals in the way of generating the initial population. During the evolution process, each individual represents a stowage scheme of the PRSS problem. In each generation, the best individual is selected according to the fitness value. Finally, from the last generation of individuals, the best individual is selected as the optimal stowage scheme of the PRSS problem.

Since the fitness calculation and evolution operations are performed for each individual, the CC at this stage is $O(PS)$.

Combining the above three stages, the CC in each generation is $O(PS*|I|^2)$. Therefore, the CC of the BRKHA is $O(PS*|I|^2*N)$, where N is the number of iterations of algorithm. Obviously, the computational cost of BRKHA is not high, since the highest degree of the polynomial $PS*|I|^2*N$ is only two.

V. COMPUTATIONAL STUDY

A. EXPERIMENTAL DESIGN

In order to test the MILP model and the proposed method, 40 instances are generated based on the actual operation of a port in the Qiongzhou Strait in China. The instances are divided into two groups according to the scale size. One

group is used to simulate the stowage problem of two small virtual passenger-cargo RoRo ships to verify the validity of the model and method. The other group chooses three kinds of actual passenger-cargo RoRo ships in the port to conduct application experiment. The instances in each group are distinguished by ship type, operation scenario, the proportion of vehicles and the number of vehicles to be packed. The distribution of vehicle proportions varies between different operating scenarios (night/daytime). According to the actual port operation, at night, there are more trucks, fewer cars and no buses. While in the daytime, there are more cars, as detailed in Table 4. Attributes of passenger-cargo RoRo ships and vehicle information are shown in Table 5 and Table 6 respectively. In addition, the parameter λ is defined to determine the number of vehicles to be packed $|I|$ based on the assumption 3), where λ is an arbitrary real number in (0, 1] in order to ensure that there are sufficient vehicles to be packed. Given a value of the parameter λ, there is a unique that meets inequalities (28) and (29) at the same time. The smaller the λ value, the larger $|I|$ is. The value of parameter λ in this paper is set to 0.5 (λ1) and 0.9 (λ2), which reflect the sufficiency of the vehicles to be packed to varying degrees.

$$\lambda \sum_{i=1}^{|I|} l_i w_i \leq LW \tag{28}$$

$$\lambda \sum_{i=1}^{|I|+1} l_i w_i > LW \tag{29}$$

The instance is named in the form of V/A-N/D-P-λ, where V/A means virtual/actual ship type, N/D means night/daytime scenario, P means vehicle proportion (divided into P1 and P2). The MILP model and the UBM are solved using the solver Gurobi 7.5 and all algorithms are coded in Python 3.6. The experimental tests are run on an Intel Core i5 Processor of 2.3 GHz with 8 GB of RAM memory running 64-bit Windows 10 operation system and all the results are the average of 10 independent runs.

B. PARAMETER SETTING

To measure the performance of proposed algorithm framework, three widely used swarm intelligence algorithms, GA [29], particle swarm optimization (PSO) [31] and whale optimization algorithm (WOA) [32], are applied separately in the evolutionary operation of the framework. The elite retention ratio in the framework is 0.1. All three algorithms set the population size to 50 and the maximum number of iterations to 100. The crossover probability in GA is 0.7 and the mutation probability is 0.2 [29]. The learning factors $c1$ and $c2$ in PSO are both set to 2, and the inertia factor is linearly decreased from 0.9 to 0.4 [31]. In WOA, convergence factor a is linearly decreased from 2 to 0 over the course of iterations, the element of random vector $\vec{r}$ is generated in [0, 1], and the probability to choose between either the shrinking encircling mechanism or the spiral model to update the position of whales is 50% [32]. For three algorithms and Gurobi, the time limit for solving each instance is set to 500 seconds.

All the three algorithms solve the PRSS problem based on the BRKHA framework, and we hence call the three algorithms BRKHGA, BRKHPSO and BRKHWOA.

C. RESULTS OF SIMULATION EXPERIMENT

The results of all methods are presented in Table 7, where f represents the utilization ratio of the cabin area, T represents the solution time, and * means the solution output when it reaches the time limit. Fig. 10 compares the results obtained by Gurobi and three algorithms in solving V2- series instances. It can be seen that for the ship V1, all methods find the optimal solution in a short time, but the Gurobi solver has a shorter solution time than other three algorithms. For the larger scale size ship V2, the Gurobi solver cannot find the optimal solution in a limited time. The output solutions of Gurobi are all inferior to those obtained by algorithms in a shorter time. Among the three algorithms, the BRKHGA is slightly superior to the other two in solving quality and time, although the solution results of three algorithms are very close.

The reasons behind the above result analysis may be as follows. Firstly, Gurobi solver is good at solving small-scale problems, but ineffective for large-scale problems. The performance of Gurobi greatly declines when handling large-scale problems. Secondly, our proposed three algorithms are based on the swarm intelligence search, which has the characteristics of self-organizing, adaptability and group-oriented, and can effectively solve large-scale instances [33]–[35].

D. RESULTS OF APPLICATION EXPERIMENT

In this section, we take three kinds of actual passenger-cargo RoRo ships as examples to conduct application experiments. Since the ship size in the application experiment is much larger than V1 and V2 in *SIMULATION EXPERIMENT* section, the Gurobi solver is not suitable for solving such high complexity problems. Here, we use Gurobi to solve the UBM, which is the relaxation model of PRSS problem, and take the solution result as the upper bound of the three algorithms. Given the complexity of the problem, we set the maximum number of iterations to 200. The experimental results of 24 instances are reported in Table 8, where u represents the upper bound obtained by Gurobi, f(avg) and f(std) respectively refer to the average value and standard deviation of cabin area utilization ratio under 10 independent runs, and the *gap*-value indicates the deviation between the f(avg) and the u. Fig. 11 and Fig. 12 show the comparison of the cabin area utilization and the *gap*-value obtained by three algorithms for solving the PRSS problem with three different sizes of ships. The value of u in the Fig. 11 is obtained by Gurobi for solving the UBM.

The results in Table 8 and Fig. 11 show that the mean cabin area utilization obtained by three algorithms all reaches a high level of 96%. As seen in Table 8 and Fig. 12, for ship A1, the *gap*-value of each algorithm is generally stable between

TABLE 7. Results of simulation experiments.

Instance	$\|I\|$	Gurobi		BRKHGA		BRKHPSO		BRKHWOA	
		f/%	T/s	f/%	T/s	f/%	T/s	f/%	T/s
V1-N-P1-λ1	9	64.13	<0.10	64.13	3.40	64.13	3.51	64.13	4.29
V1-N-P1-λ2	5	64.05	<0.10	64.05	2.59	64.05	2.75	64.06	3.38
V1-N-P2-λ1	11	72.32	0.81	72.32	4.14	72.32	4.44	72.32	5.75
V1-N-P2-λ2	6	63.06	0.11	63.06	3.20	63.06	3.42	63.06	4.04
V1-D-P1-λ1	12	81.75	0.50	81.75	4.09	81.75	4.42	81.75	5.33
V1-D-P1-λ2	7	70.23	<0.10	70.23	3.50	70.23	3.69	70.23	4.45
V1-D-P2-λ1	12	71.09	1.49	71.09	4.46	71.09	4.74	71.09	5.90
V1-D-P2-λ2	8	70.00	0.12	70.00	3.87	70.00	4.02	70.00	4.74
V2-N-P1-λ1	57	85.15*	500.00	88.33	45.92	88.08	47.92	88.08	54.26
V2-N-P1-λ2	32	87.71*	500.00	89.44	24.68	89.44	27.34	89.44	27.75
V2-N-P2-λ1	59	86.60*	500.00	89.02	47.99	89.02	51.61	89.02	64.11
V2-N-P2-λ2	34	87.22*	500.00	88.49	27.90	88.49	30.94	88.49	32.23
V2-D-P1-λ1	65	82.86*	500.00	89.35	49.05	88.59	52.32	88.95	63.57
V2-D-P1-λ2	40	85.05*	500.00	88.00	34.74	88.00	37.98	88.00	40.77
V2-D-P2-λ1	79	84.59*	500.00	90.00	70.05	89.83	81.93	90.00	92.78
V2-D-P2-λ2	44	85.06*	500.00	90.25	38.60	89.87	40.58	89.67	57.48
Average	-	77.55	250.19	79.34	23.01	79.25	25.10	79.27	29.43

TABLE 8. Results of application experiments.

Instance	$\|I\|$	u	BRKHGA			BRKHPSO			BRKHWOA		
		f/%	f(avg)/%	f(std)	gap/%	f(avg)/%	f(std)	gap/%	f(avg)/%	f(std)	gap/%
A1-N-P1-λ1	136	100.00	96.92	1.68e-03	3.08	96.69	1.32e-03	3.31	96.69	9.87e-04	3.31
A1-N-P1-λ2	77	100.00	96.56	3.00e-03	3.44	96.37	1.20e-03	3.63	96.23	2.87e-03	3.77
A1-N-P2-λ1	154	100.00	97.04	1.53e-03	2.96	96.78	1.13e-03	3.22	96.77	1.83e-03	3.23
A1-N-P2-λ2	86	100.00	96.27	1.57e-03	3.77	96.12	1.95e-03	3.86	96.10	2.95e-03	3.90
A1-D-P1-λ1	177	99.99	97.47	5.04e-03	2.52	97.40	7.97e-03	2.59	97.32	6.16e-03	2.67
A1-D-P1-λ2	97	99.99	96.92	1.45e-03	3.07	96.85	3.30e-03	3.14	96.69	6.55e-04	3.06
A1-D-P2-λ1	189	100.00	96.90	4.51e-03	3.10	96.50	4.46e-03	3.51	96.29	5.56e-03	3.71
A1-D-P2-λ2	104	99.99	96.93	3.08e-03	3.06	96.45	4.05e-03	3.54	96.68	3.76e-03	3.31
A2-N-P1-λ1	200	99.99	93.90	4.16e-03	6.09	93.99	1.47e-03	6.00	93.56	1.90e-03	6.43
A2-N-P1-λ2	115	100.00	94.46	1.68e-03	5.54	94.34	8.95e-04	5.62	94.25	1.96e-03	5.75
A2-N-P2-λ1	221	99.99	96.41	1.45e-03	3.58	96.52	4.03e-03	3.47	96.12	2.41e-03	3.87
A2-N-P2-λ2	121	99.91	95.55	2.35e-03	4.36	95.29	1.36e-03	4.62	94.98	3.01e-03	4.94
A2-D-P1-λ1	255	99.99	97.64	2.07e-03	2.35	97.55	1.83e-03	2.44	97.40	3.83e-03	2.59
A2-D-P1-λ2	137	99.99	97.91	1.17e-03	2.08	98.11	3.52e-03	1.88	97.82	1.73e-03	2.17
A2-D-P2-λ1	279	100.00	98.14	1.28e-03	1.86	97.62	2.98e-03	2.38	97.84	5.82e-03	2.16
A2-D-P2-λ2	165	100.00	97.92	2.65e-03	2.08	97.89	3.56e-03	2.11	98.13	4.06e-03	1.87
A3-N-P1-λ1	216	99.99	94.60	2.23e-03	5.39	94.41	9.57e-04	5.58	94.29	7.29e-04	5.70
A3-N-P1-λ2	118	99.99	94.27	6.27e-04	5.72	94.19	1.04e-03	5.80	94.16	1.91e-03	5.83
A3-N-P2-λ1	239	100.00	95.86	1.47e-03	4.14	95.73	1.36e-03	4.27	95.72	9.98e-04	4.28
A3-N-P2-λ2	134	99.99	95.86	1.24e-03	4.14	96.04	1.84e-03	3.95	95.81	9.94e-04	4.18
A3-D-P1-λ1	263	99.99	97.45	3.12e-03	2.54	97.10	3.48e-03	2.89	97.35	1.42e-03	2.64
A3-D-P1-λ2	152	99.99	98.35	3.58e-03	1.65	98.40	3.63e-03	1.59	97.82	2.14e-03	2.17
A3-D-P2-λ1	309	100.00	98.22	9.08e-04	1.78	97.84	2.54e-03	2.16	97.68	3.24e-03	2.32
A3-D-P2-λ2	167	100.00	97.78	4.01e-03	2.22	97.42	3.73e-03	2.58	97.08	3.07e-03	2.92
Average	-	99.99	96.64	2.33e-03	3.36	96.48	2.65e-03	3.51	96.37	2.67e-03	3.62

2.5% and 3.8%. For ships A2 and A3, as the proportion of cars increases, the *gap*-value overall drops from 6.5% to 1.5% with a downward trend. The reason for the difference of *gap*-value trend among three ships can be attributed to the following facts. Firstly, compared to the ship A1, the A2 and A3 ships are wider, which results in the gap created by the placed trucks being able to accommodate a wider variety of cars. Therefore, the range of *gap*-value of ships A2 and A3 is larger than that of A1. Then, the proportion of cars arriving at the port in the daytime is higher than that at night. As the proportion of cars increases, the utilization rate of the gaps in ships A2 and A3 gradually increases. Thus, in the experiment, as the scenario changes from night to daytime, the *gap*-value of ships A2 and A3 gradually decreases.

To make the experimental results more convincing, we use Kruskal-Wallis ANOVA method [34]–[36] with the significance level of 0.05 to analyze the difference of the three algorithms. Fig. 13 shows the significance test results for three algorithms under PRSS problem. It is clear that all the p-values are more than 0.05, which means there are no significant differences among these three algorithms during the solution of instances from the perspective of statistical analysis. Furthermore, the sample median line of the mean area utilization (the red line segment shown in Fig. 13(a)) of BRKHGA is the highest, and the sample median lines

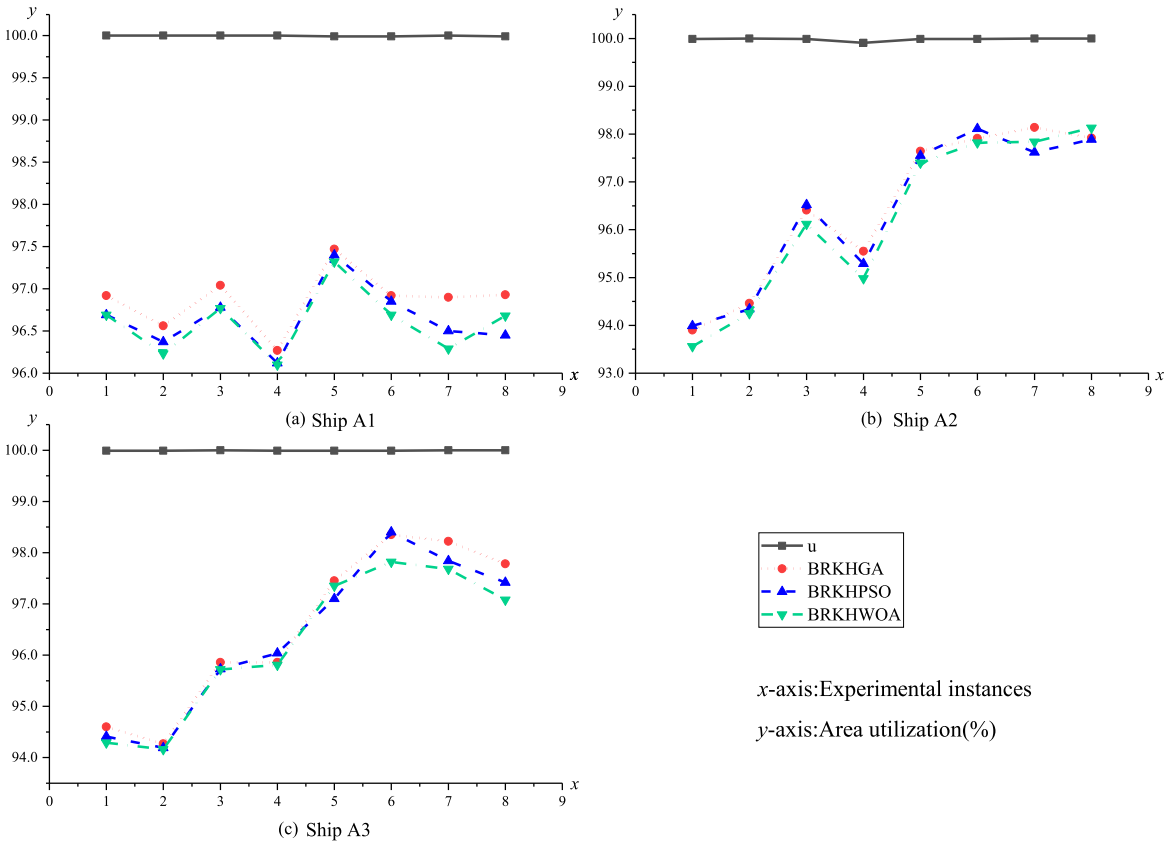

FIGURE 11. Visual comparison of ships A1∼A3 stowage area utilization.

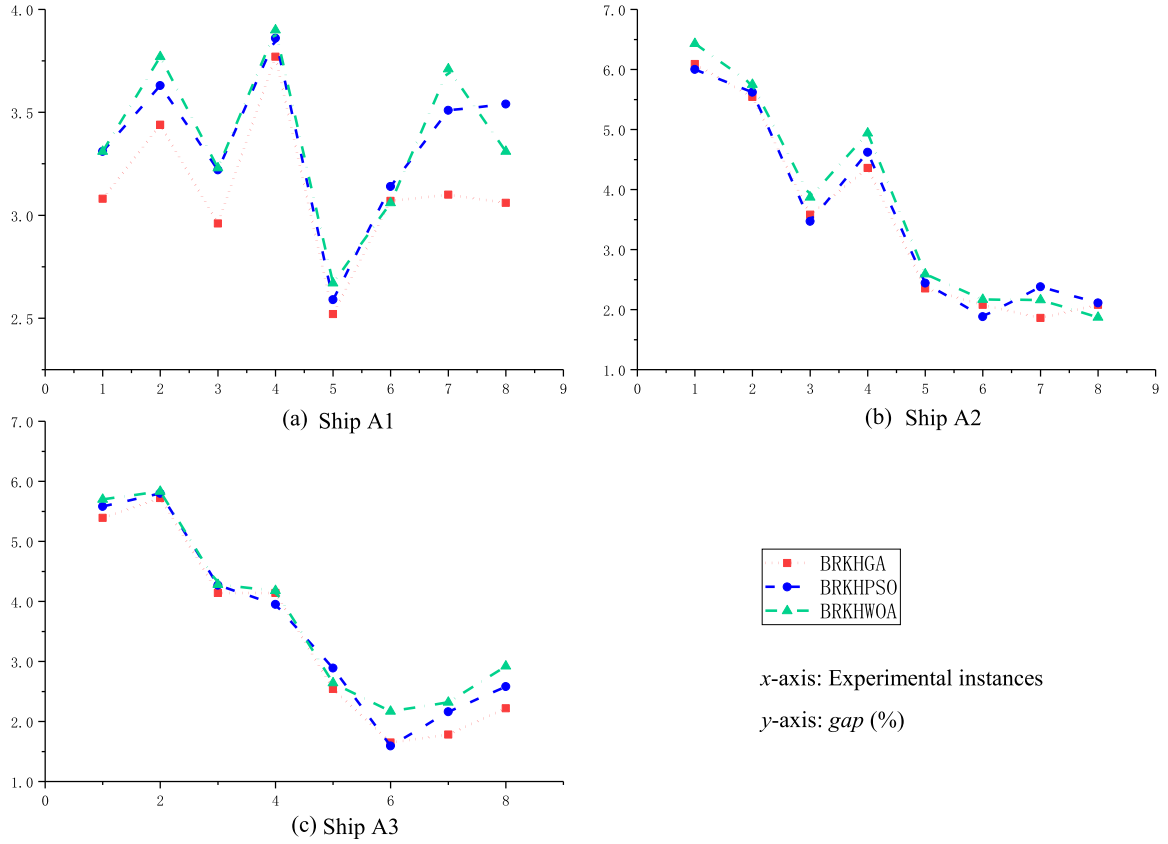

FIGURE 12. Visual comparison of ships A1∼A3 *gap*-value.

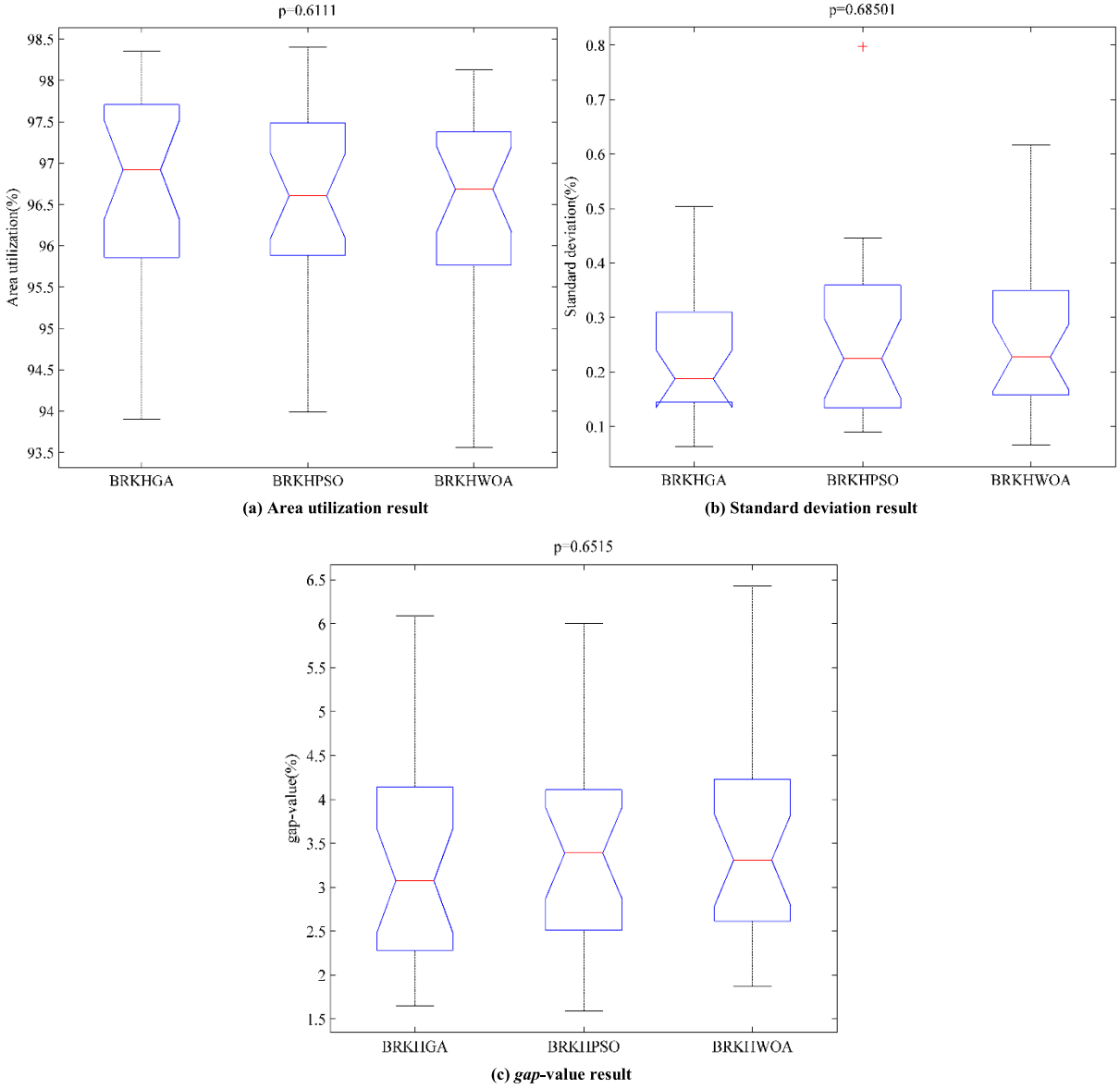

FIGURE 13. Kruskal-Wallis ANOVA significance test results for three algorithms under PRSS problem.

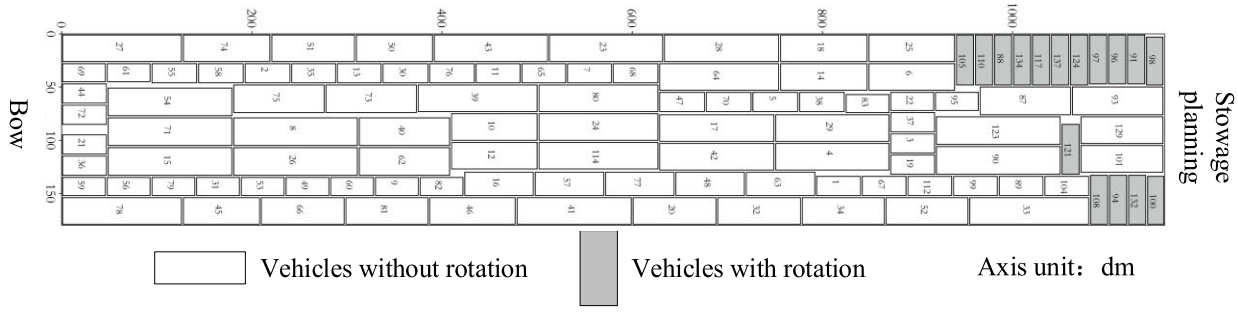

FIGURE 14. Visual display of stowage scheme obtained by BRKHGA.

of the mean standard deviation (the red line segment shown in Fig. 13(b)) and the mean *gap*-value (the red line segment shown in Fig. 13(c)) of BRKHGA are both the lowest. It is obvious that the performance of BRKHGA is the best among the three algorithms, which is consistent with the result analysis in Table 8, Fig. 11 and Fig. 12.

In summary, for three typical passenger-cargo RoRo ships, the cabin area utilization obtained by three algorithms generally exceed 95%, and the average *gap*-value and average standard deviation remain at a low level. Moreover, there is no significant difference among these three algorithms during the solution of instances, and the performance of BRKHGA is slightly prominent. The reason may be that all three algorithms are based on the same framework. In other words, the evolutionary operations in the framework show the following advantages: 1) evolutionary operation has strong robustness, self-organizing, adaptability and group-oriented characteristics which play an important role in the solution. 2) Multiple individuals will be generated with evolutionary operation, which increases the population diversity and avoids the algorithm falling into local optimum. The only difference in the three algorithms is the evolutionary search mechanism. Based on the experiment results, GA's evolutionary search mechanism may be a better choice for the proposed algorithm framework in addressing the PRSS.

In order to visualize stowage scheme, Fig. 14 shows one of the solutions of the instance A2-D-P1-λ2. The numbers in the rectangles indicate the order in which the vehicle arriving at the area to be loaded.

VI. CONCLUSION

This paper studies the PRSS problem with the objective to maximize the cabin area utilization of the ship considering the characteristics of two-dimensional packing, two-phase, rotation and safe navigation. The corresponding MILP model is formulated. The BRKHA framework consisting of encoding, multi-phase heuristic and swarm intelligence search based evolutionary operation is proposed to solve the problem. GA, PSO and WOA are applied separately in the evolutionary operation of the framework. Based on the data of a port in the Qiongzhou Strait in China, the simulation experiment and application experiment are designed respectively to verify the validity of the model and the algorithm framework. The results prove that all three algorithms based on the BRKHA framework are well suited to solve the PRSS problem. Moreover, the Kruskal-Wallis ANOVA test indicates that the performance of BRKHGA is the best one, although there is no significant difference among these three algorithms. In conclusion, the research of this paper is helpful for the realization of intelligent stowage decision-making using computer software.

This study has opened up several directions for future investigations. Firstly, more efficient solutions could be obtained by improving heuristics designed in this paper. Secondly, the proposed BRKHA framework may be further integrated with other state-of-the-art optimization algorithms to test its performance. Finally, the dynamic vehicle information should be considered in extended study of PRSS problem.

ACKNOWLEDGMENT

The authors would like to thank the anonymous reviewers for their valuable comments and suggestions to improve the quality of this article.

CONFLICTS OF INTEREST

The authors declare no conflict of interest.

REFERENCES

[1] B.-O. Øvstebø, L.-M. Hvattum, and K. Fagerholt, "Routing and scheduling of RoRo ships with stowage constraints," *Trans. Res. C, Emerg. Technol.*, vol. 19, no. 6, pp. 1225–1242, Feb. 2011.

[2] C. Kroer, M. K. Svendsen, R. M. Jensen, J. Kiniry, and E. Leknes, "Symbolic configuration for interactive container ship stowage planning," *Comput. Intell.*, vol. 32, no. 2, pp. 259–283, May 2016.

[3] M. F. Monaco, M. Sammarra, and G. Sorrentino, "The terminal-oriented ship stowage planning problem," *Eur. J. Oper. Res.*, vol. 239, no. 1, pp. 256–265, Nov. 2014.

[4] J. Li, Y. Zhang, and S.-Y. Ji, "Multi-stage hierarchical decomposition approach for stowage planning problem in inland container liner shipping," *J. Oper. Res. Soc.*, vol. 2, pp. 1–19, Dec. 2019.

[5] J. Li, Y. Zhang, J. Ma, and S. Ji, "Multi-port stowage planning for inland container liner shipping considering weight uncertainties," *IEEE Access*, vol. 6, pp. 66468–66480, 2018.

[6] J. Li, Y. Zhang, and S.-Y. Ji, "Inland container liner route stowage planning decision with uncertain container weight," *J. Trans. Syst. Eng. Inf. Technol.*, vol. 18, no. 2, pp. 208–215, Apr. 2018, doi: 10.16097/j.cnki.1009-6744.2018.02.031.

[7] N. Zhao, Y.-C. Guo, and T.-Y. Xiang, "Container ship stowage based on Monte Carlo tree search," *J. Coastal Res.*, vol. 83, pp. 540–547, Feb. 2018.

[8] Z. Wei-Ying, L. Yan, and J. Zhuo-Shang, "Model and algorithm for container ship stowage planning based on bin-packing problem," *J. Mar. Sci. Appl.*, vol. 4, no. 3, pp. 30–36, Sep. 2005.

[9] J.-J. Wei, "A new algorithm for container ship's stowage," presented at the 21th Int. Conf. Artif. Intell., Hainan Island, China, Apr. 2009.

[10] A. Sciomachen and E. Tanfani, "A 3D-BPP approach for optimising stowage plans and terminal productivity," *Eur. J. Oper. Res.*, vol. 183, no. 3, pp. 1433–1446, Dec. 2007.

[11] T. Umeda, A. Kitamura, M. Konishi, S. Kanamura, and S. Takami, "Optimiation search algorithm of allocation planning for strip coils in hold for shipment by using operational know-how.," *ISIJ Int.*, vol. 41, no. 5, pp. 446–453, 2001.

[12] L. Tang, J. Liu, F. Yang, F. Li, and K. Li, "Modeling and solution for the ship stowage planning problem of coils in the steel industry," *Nav. Res. Logistics*, vol. 62, no. 7, pp. 564–581, Oct. 2015.

[13] B. O. Øvstebø, L. M. Hvattum, and K. Fagerholt, "Optimization of stowage plans for RoRo ships," *Comput. Oper. Res.*, vol. 38, no. 10, pp. 1425–1434, Oct. 2011.

[14] J.-R. Hansen, I. Hukkelberg, and K. Fagerholt, "2D-packing with an application to stowage in roll-on roll-off liner shipping," presented at the 12th Int. Conf. Comput. Logist., Lisbon, Portugal, Sep. 2016.

[15] R. R. Amossen and D. Pisinger, "Multi-dimensional bin packing problems with guillotine constraints," *Comput. Oper. Res.*, vol. 37, no. 11, pp. 1999–2006, Nov. 2010.

[16] P. M. Castro and J. F. Oliveira, "Scheduling inspired models for two-dimensional packing problems," *Eur. J. Oper. Res.*, vol. 215, no. 1, pp. 45–56, Nov. 2011.

[17] A. Lodi, S. Martello, and D. Vigo, "Heuristic and Metaheuristic approaches for a class of two-dimensional bin packing problems," *Informs J. Comput.*, vol. 11, no. 4, pp. 345–357, Nov. 1999.

[18] S. C. H. Leung, D. Zhang, C. Zhou, and T. Wu, "A hybrid simulated annealing Metaheuristic algorithm for the two-dimensional knapsack packing problem," *Comput. Oper. Res.*, vol. 39, no. 1, pp. 64–73, Jan. 2012.

[19] K. Shiangjen, J. Chaijaruwanich, and W. Srisujjalertwaja, "Enhancing the efficiency of heuristic placement algorithm for two-dimensional orthogonal knapsack packing problem," presented at the 6th Int. Conf. Software Eng. Serv. Sci., Beijing, China, Sep. 2015.

[20] L. Wei, Q. Hu, S. C. H. Leung, and N. Zhang, "An improved skyline based heuristic for the 2D strip packing problem and its efficient implementation," *Comput. Oper. Res.*, vol. 80, pp. 113–127, Apr. 2017.

[21] E. K. Burke, G. Kendall, and G. Whitwell, "A new placement heuristic for the orthogonal stock-cutting problem," *Oper. Res.*, vol. 52, no. 4, pp. 655–671, Aug. 2004.
[22] S. Zhou, X. Li, K. Zhang, and N. Du, "Two-dimensional knapsack-block packing problem," *Appl. Math. Model.*, vol. 73, pp. 1–18, Sep. 2019.
[23] R. Lahyani, K. Chebil, M. Khemakhem, and L. C. Coelho, "Matheuristics for solving the multiple knapsack problem with setup," *Comput. Ind. Eng.*, vol. 129, pp. 76–89, Mar. 2019.
[24] S. Martello and M. Monaci, "Algorithmic approaches to the multiple knapsack assignment problem," *Omega*, vol. 90, pp. 1–11, Nov. 2020.
[25] M. Dell'Amico, M. Delorme, M. Iori, and S. Martello, "Mathematical models and decomposition methods for the multiple knapsack problem," *Eur. J. Oper. Res.*, vol. 274, no. 3, pp. 886–899, May 2019.
[26] A. Bortfeldt and G. Wäscher, "Constraints in container loading—A state-of-the-art review," *Eur. J. Oper. Res.*, vol. 229, no. 1, pp. 1–20, Aug. 2013.
[27] J. Olsson, T. Larsson, and N.-H. Quttineh, "Automating the planning of container loading for Atlas Copco: Coping with real-life stacking and stability constraints," *Eur. J. Oper. Res.*, vol. 280, no. 3, pp. 1018–1034, Feb. 2020.
[28] Y. Lan, G. Dósa, X. Han, C. Zhou, and A. Benko, "2D knapsack: Packing squares," *Theor. Comput. Sci.*, vol. 508, pp. 35–40, Oct. 2013.
[29] J. F. Gonçalves and M. G. C. Resende, "Biased random-key genetic algorithms for combinatorial optimization," *J. Heuristics*, vol. 17, no. 5, pp. 487–525, Oct. 2011.
[30] X.-S. Yang, S. Deb, Y.-X. Zhao, S. Fong, and X. He, "Swarm intelligence: Past, present and future," *Soft Comput.*, vol. 22, no. 18, pp. 5923–5933, Sep. 2018.
[31] Y.-H. Shi and R.-C. Eberhart, "A modified particle swarm optimizer," in *Proc. IEEE ICEC Conf.*, Anchorage, AK, USA, May 1998, pp. 69–73.
[32] S. Mirjalili and A. Lewis, "The whale optimization algorithm," *Adv. Eng. Softw.*, vol. 95, pp. 51–67, May 2016.
[33] L.-J. He, W.-F. Li, and Y. Zhang, "Review of swarm intelligence algorithms for multi-objective flowshop scheduling," in *Proc. 11th Int. Conf. Internet Distrib. Comput. Syst.*, Tokyo, Japan, 2018, pp. 258–269.
[34] L. He, W. Li, Y. Zhang, and Y. Cao, "A discrete multi-objective fireworks algorithm for flowshop scheduling with sequence-dependent setup times," *Swarm Evol. Comput.*, vol. 51, Dec. 2019, Art. no. 100575, doi: 10.1016/j.swevo.2019.100575.
[35] L.-J. He, W.-F. Li, and Y. Zhang, "Multi-objective optimization method based on grey synthetic incidence analysis," (in Chinese), *Control Decis.*, vol. 35, no. 5, pp. 1134–1142, 2020, doi: 10.13195/j.kzyjc.2018.0904.
[36] G.-Y. Zhu, L.-J. He, X.-W. Ju, and W.-B. Zhang, "A fitness assignment strategy based on the grey and entropy parallel analysis and its application to MOEA," *Eur. J. Oper. Res.*, vol. 265, no. 3, pp. 813–828, Mar. 2018.
[37] L. Yang, Y. Zhang, R. Chiong, S. Dhakal, and Q. Qi, "Using evolutionary game theory to study behavioral strategies of the government and carriers under different transshipment modes," *IEEE Access*, vol. 8, pp. 18514–18521, 2020.

YU ZHANG received the Ph.D. degree from the School of Logistics Engineering, Wuhan University of Technology, Wuhan, China, in 2007. He is currently a Professor with the Wuhan University of Technology. His research interests include supply chain management, optimization, and the development of mathematical modeling and algorithms.

HONGWEI TIAN received the M.Sc. degree from the School of Automobile and Traffic Engineering, Wuhan University of Science and Technology, Wuhan, China, in 2019. He is currently pursuing the Ph.D. degree with the School of Logistics Engineering, Wuhan University of Technology. His current research interests include waterway transportation and optimization algorithms.

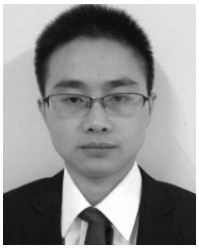

LIJUN HE received the B.S. degree in mechanical and electronic engineering from the Nanjing Institute of Technology, China, in 2012, and the M.S. degree in mechanical design and theory from Fuzhou University, China, in 2016. He is currently pursuing the Ph.D. degree with the School of Logistics Engineering, Wuhan University of Technology, Wuhan, China. His current research interests include multiobjective optimization and production scheduling.

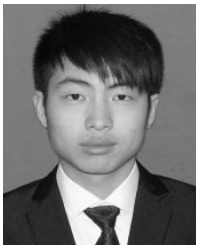

SHAOKANG MA received the B.S. degree from the School of Automobile and Traffic Engineering, Wuhan University of Science and Technology, Wuhan, China, in 2019. He is currently pursuing the M.Sc. degree with the School of Logistics Engineering, Wuhan University of Technology. His current research interests include system optimization and simulation, and water transport engineering.

LIJUAN YANG received the M.S. degree from the Transportation College, Jilin University, China. She is currently pursuing the Ph.D. degree with the Wuhan University of Technology, China. Her research interests include inland waterway transportation, lock scheduling, multimodal transportation, and game models.